Grundwasser – Zeitschrift der Fachsektion Hydrogeologie (2016) 21:29–41
DOI 10.1007/s00767-015-0313-9

FACHBEITRAG

Fault controlled geochemical properties in Lahendong geothermal reservoir Indonesia

Maren Brehme[1] · Fiorenza Deon[1] · Christoph Haase[2] · Bettina Wiegand[3] · Yustin Kamah[4] · Martin Sauter[3] · Simona Regenspurg[1]

Eingang des Beitrages: 29.5.2015 / Eingang des überarbeiteten Beitrages: 23.9.2015 / Online veröffentlicht: 15.2.2016

Abstract Rock and fluid geochemical data from Lahendong, Indonesia, were analyzed to evaluate the influence of fault zones on reservoir properties. It was found that these properties depend on fault-permeability controlled fluid flow.

Results from measurements of spring and well water as well as rocks and their hydraulic properties were combined with hydrochemical numerical modeling. The models show that the geothermal field consists of two geochemically distinct reservoir sections. One section is characterized by acidic water, considerable gas discharge and high geothermal-power productivity—all related to increased fault zone permeability. The other section is characterized by neutral water and lower productivity.

Increased fluid flow in the highly fractured and permeable areas enhances chemical reaction rates. This results in strong alteration of their surrounding rocks. Numerical models of reactions between water and rock at Lahendong indicate the main alteration products are clay minerals. A geochemical conceptual model illustrates the relation between geochemistry and permeability and their distribution within the area.

Our conceptual model illustrates the relation between geochemistry and fault-zone permeability within the Lahendong area. Further mapping of fault-related permeability would support sustainable energy exploitation by avoiding low-productive wells or the production of highly corroding waters, both there and elsewhere in the world.

Keywords Hydrochemistry · Alteration · Subsurface fluid-flow · Fault-permeability · Structural controls · Hydrogeology

✉ Maren Brehme
brehme@gfz-potsdam.de

Fiorenza Deon
fdeon@gfz-potsdam.de

Christoph Haase
haase02@googlemail.com

Bettina Wiegand
bwiegan@gwdg.de

Yustin Kamah
yustinkamah@pertamina.com

Martin Sauter
martin.sauter@geo.uni-goettingen.de

Simona Regenspurg
regens@gfz-potsdam.de

[1] Helmholtz Centre Potsdam – GFZ German Research Centre for Geosciences, International Centre for Geothermal Research, Telegrafenberg, 14473 Potsdam, Germany

[2] Institute for Geosciences, Kiel University, Ludewig-Meyn-Straße 10, 24118 Kiel, Germany

[3] Applied Geology, University of Göttingen, Goldschmidtstraße 3, 37077 Göttingen, Germany

[4] Upstream Technology Center Pertamina, Jl. Medan Merdeka Timur no.6, Jakarta, Indonesia

Durch Störungszonen kontrollierte geochemische Eigenschaften des geothermischen Reservoirs Lahendong in Indonesien

Zusammenfassung Die Analyse von geochemischen Daten am Standort Lahendong in Indonesien wird in dieser Studie für die Untersuchung des Einflusses von Störungszonen auf Reservoireigenschaften genutzt. Diese Eigenschaften sind von Grundwasserbewegungen in Störungszonen und deren Permeabilitäten abhängig.

In unserem Ansatz werden die Ergebnisse von physikochemikalischen Messungen an Brunnen und Quellen, Laboruntersuchungen zur Zusammensetzung von Wasser und Gesteinen und deren hydraulische Eigenschaften mit den Resultaten aus hydrochemischen Simulationen kombiniert. Die Ergebnisse zeigen, dass das geothermische Feld aus zwei geochemisch unterschiedlichen Reservoirbereichen besteht, wovon eins durch saures Wasser, erhöhte Gasaustritte und höhere Produktionsraten charakterisiert ist und das andere durch neutrale Wässer charakterisiert ist. Durch intensive Grundwasserbewegungen und chemische Reaktionen in Störungszonen, weisen Gesteine vor allem in diesen Bereichen starke Alterationserscheinungen auf. Die chemischen Reaktionen zwischen Wasser und Gestein wurden durch numerische Simulationen abgebildet und zeigen, dass durch die Alterationsprozesse vor allem Tonminerale gebildet werden. Ein konzeptionelles Modell stellt den Zusammenhang zwischen geochemischen Eigenschaften und der Permeabilitätsverteilung im Gebiet dar.

Unser konzeptionelles Modell erklärt den Zusammenhang zwischen Geochemie und Permeabilitäten in Störungszonen in Lahendong. Die Untersuchung von Permeabilitätsverteilungen in geothermischen Reservoiren ist wichtig für eine nachhaltige Nutzung und verhindert das Bohren an unproduktiven Standorten, sowie die Förderung von sauren, aggressiven Wässern in Lahendong und vergleichbaren Standorten.

Geochemical features provide reliable constrains for the permeability of faulted areas. The aim of this study was to identify permeability-rich faulted areas based on geochemical properties of rocks and fluids at Lahendong. This high-enthalpy geothermal field, located in Northern Sulawesi, Indonesia, is operated by P.T. Pertamina Geothermal Energy. The field has an installed capacity of 80 MW_e, which is sustained by 8,300 tons of steam per day from 10 production wells. The Lahendong reservoir is composed of basaltic andesites, tuff, and volcanic breccia that were intruded by diorites at some locations (Siahaan et al. 2005; Utami 2011). Geochemical investigations were started there in the early 1970s (Surachman et al. 1987), but the evolution and distribution of thermal fluids is still under debate.

A new conceptual model has recently been proposed for the area and is summarized here in Fig. 1 (Brehme et al. 2013, 2014; Koestono 2010; Wiegand et al. 2013).

This Figure suggests that the geothermal field consists of two sub-reservoirs, which are separated by an area of fault-parallel permeable versus fault-perpendicular less permeable zone. In the area hot springs often discharge along or at the junction of conjugate faults. In the northern part of the study area wells and hot springs are characterized by low pH values, while more neutral pH fluids are found in the southern and eastern margin. Production rates vary between the northern and southern parts by a factor of five, with highest productivities in the North.

Introduction

In some parts of the world geothermal power is an indispensable component of renewable energy resources. Efficient utilization of this component requires effective geological, geochemical, and geophysical approaches to resource characterization to optimize the reservoir performance. Geochemical data are often used as an instrument to interpret the potential of a geothermal field, because they indicate the geothermal field size, subsurface temperatures, and rock compositions (Arnorsson 2000). In this study, geochemical investigations on brine and reservoir rocks were performed to evaluate the influence of fault zones on reservoir properties.

Sustainable geothermal use requires understanding of the reservoir's geochemical characteristics. Acidic fluids constitute high risks for the thermal fluid loop because low pH-water enhances corrosion of pipes and casing, decreasing the stability of geothermal plant components (Corsi 1986). The geochemical properties, in turn, are strongly influenced by subsurface fluid flow. At Lahendong we show that these flows are mainly controlled by permeable and impermeable faults in tectonically active areas.

Methods

Water sampling and analysis

Water samples were collected from ten 1800 m deep production wells targeting the reservoir and from eleven hot springs in the Lahendong area (Fig. 1). Well samples were extracted from a brine-and-steam mixture at the wellheads using a *mini-separator* that keeps the fluid at pipe pressure without heat loss (Truesdell et al. 1987). Sampling was done according to hydrogeological standard procedures (Brehme et al. 2010). After on-site pH, electric conductivity (EC), temperature (T), and bicarbonate (HCO_3) tests, the brine was filtered to <0.45 µm and acidified to pH <2 using HCl.

The resulting fluid element-concentrations were then analyzed by inductively coupled plasma atomic emission spectroscopy using a Varian VISTA-MPX ICP-AES and Dionex ICS System3000 ion chromatography machines. Quantitatively analyzed elements are Ca, Fe, K, Mg, Mn, Na, Si (given here as silicic acid H_4SiO_4), Sr, Zn, Li, B, Ba, Al, Cs, and As (using ICP-AES) and F, Cl, NO_2, Br, NO_3, SO_4, and PO_4 (using ICS). In the figures and tables summarizing these measurements, green and blue colors were used to depict acidic versus neutral waters.

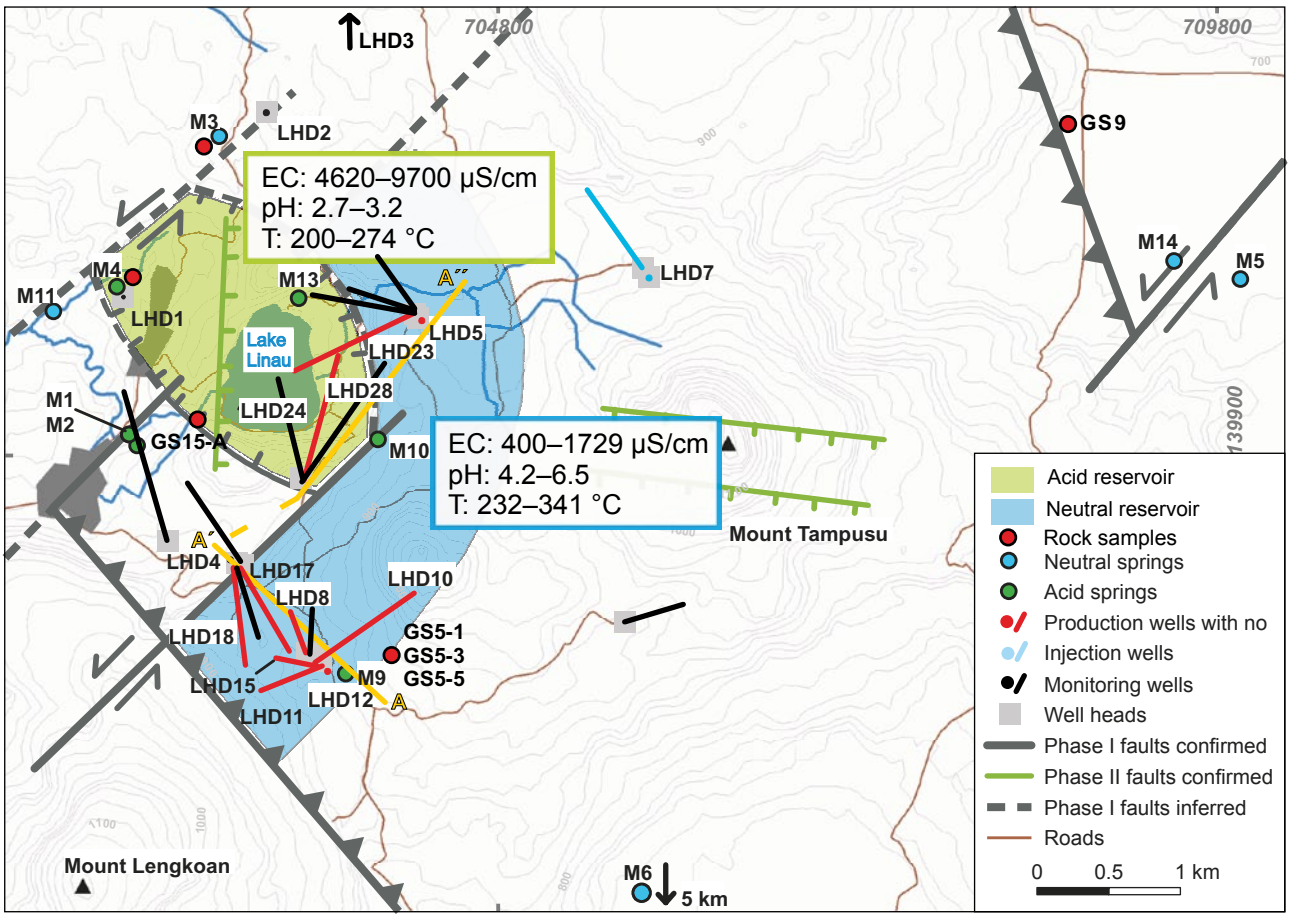

Fig. 1 Map of the study area with main faults and hydrochemical characteristics (*EC* electrical conductivity, *T* temperature). *Red, blue, and black lines* indicate deviated wells. The *yellow line* shows the location of the cross section in Fig. 5. Water sample analyses are given in Table 1 and 2 and rock sample analysis in Tables 3, 4, 5, 6, 7, 8 and Fig. 4 (modified from Brehme et al. 2014)

Rock sampling and analysis

Rock samples were taken from wellbore-cores, outcrops and areas of rising hot springs in the Lahendong area (Fig. 1). Surface rock samples from outcrops were analyzed by X-ray diffraction (XRD) and X-ray fluorescence (XRF). To quantify mineral composition, the rock samples were crushed and sieved to < 63 µm. Powder XRD patterns were recorded by a fully automated STOE STADI P diffractometer.

The diffractogram interpretations were refined using the EXPGUI-GSAS method (Belsky et al. 2002; Larson and Von Dreele 2004; Toby 2001) and reference crystal structures from the ICDS database (Bergerhof and Brown 1987). This refinement allows a semi-quantitative determination of minerals in a rock sample with an accuracy of up to 5 wt. %. The clay mineral fraction was determined qualitatively. The XRD pattern was evaluated with the EVA diffraction suite method (Giencke 2007).

The XRF analysis was performed on a Bruker S4 Pioneer instrument, equipped with a 4 kW Rh tube. Details about the measurement conditions and refinement procedures are described in Deon et al. (2015, 2013).

Permeability

Matrix permeabilities were measured on 5 cm × 5 cm × 2.5 cm cylindrical specimens taken parallel to the bedding of wellbore-cores from different parts of the study area. The experimental set-up was a conventional gas-permeameter as described by Milsch et al. (2011). It consists of a pressure vessel, a core holder with jacket, pressure gages for confining, up- and downstream pressure and flow meters. Argon was used as inert gas for 55 bar confining and pore pressure, the latter being increased stepwise throughout the experiment from 17, 27, 37, 47 bar. Results were adjusted with the Klinkenberg-correction following Tanikawa and Shimamoto (2009).

Geochemical modelling

The geochemical code PHREEQC, in combination with the phreeqc.dat database, allows calculating pressure effects on the equilibrium constants of reactions from at least 0 to 200 °C and 1 to 1000 atm (Parkurst et al. 1980, Parkhurst and Appelo 2013; Appelo et al. 2015). The code was applied to calculate the reaction of gas phases with the solutions at equilibrium using the Peng-Robinson's state equation (Robinson et al. 1985).

The aim of the numerical modeling was to predict supersaturation (SI) and potential precipitation and dissolution processes under reservoir conditions. In the first step, measured reservoir water composition was adapted to the predominant in-situ pressure, temperature, and gas phase conditions. Under them, certain minerals were identified to be supersaturated in the reservoir water. In a second step, these mineral phases were set into equilibrium with the reservoir water and were allowed to precipitate, thus showing if minerals are in equilibrium or still supersaturated in reservoir water.

In order to understand the origin of spring waters, modeling should be based on reservoir water composition. Hot spring water composition was calculated by mixing reservoir water with cold low salinity water in a ratio of 1 to 10, thus adjusting them to the observed temperature of their hot springs. This factor was estimated from the average difference of Cl^- concentrations in hot spring and reservoir water. Modeling also included the degassing of CO_2 and H_2S at atmospheric conditions and subsequent equilibration with O_2. Neutral and acidic waters were equilibrated with supersaturated silica-minerals. After these steps, supersaturated minerals were assumed to precipitate at the prevailing conditions. Finally, these simulated precipitated mineral phases were compared with observed minerals from surface and subsurface samples.

Results

Liquid samples

In general, water from wells and hot springs was found to be either highly acidic (pH of 1.8–3.2) or noticeably closer to neutral (pH of 4.2–7.0). The reservoir waters can be classified as chloride or acid sulphate-chloride types, while hot springs are bicarbonate- or sulphate water types (Table 1, 2; Arnorsson et al. 2007; Ellis and Mahon 1977; Nicholson 1993; Utami 2011 and White 1957). Ion balances of reservoir and hot spring water range between 0 and 47% (Table 1, 2). These balances show a strong excess of cations for the wells and neutral springs as compared to 28–93% excess of anions, especially sulphate, for the acid springs.

Table 1 Hydrochemical composition of well water

Sample name	Liquid phase																									Gas phase		Permeable zone from to (m) TVD	Ion balance (%)
	EC (µS/cm)	pH	T	RES	HCO_3^-	F^-	Cl^-	NO_2^-	Br^-	NO_3^-	SO_4^{2-}	PO_4^{3-}	Ca^{2+}	$Fe^{2+/3+}$	K^+	Mg^{2+}	Mn^{2+}	Na^+	H_4SiO_4	Sr^{2+}	Zn^{2+}	Li^{1+}	B^{3+}	Ba^{2+}	Al	Cs^{1+}	As	CO_2	H_2S		
LHD 5	400	4.2	232	6		0.1	12	<0.15	<0.1	0.10	17	1.3		4.5	<10	0.69	<0.1	20	15	<0.1	0.9	0.04	1.1	0.00024	3.28	0.01	0.14	134	9	1550	1700	18
LHD 8	1729	6.5	316	68		3.4	348	<0.15	1.42	<0.1	114	<0.1	2.9	0.7	27	0.13	<0.1	316	163	0.01	1.3	0.24	8.9	0.00063	0.92	0.25	2.20	126	23	1156	1318	11
LHD 10	1533	6	308	64		1.5	295		1.08	<0.1	109	<0.1	7.4	0.6	45	<0.1	<0.1	228	218	0.03	<0.1	0.58	3.1	0.00079	0.56			134	23	1837	1905	5
LHD 11	972	5.9	312	29		1.0	215	<0.15	0.72	<0.1	52	<0.1	4.4	1.0	31	0.52	<0.1	174	146	0.01	2.0	0.58	3.1	0.00042	1.88	1.08	3.98	114	30	1266	1542	10
LHD 12	1541	5.3	327	23		1.4	452	<0.15	1.59	<0.1	46	<0.1	3.8	0.7	80	0.15	<0.1	282	322	0.01	0.7	1.50	4.3	0.00067	1.27	1.24	1.40	75	22	1500	1800	4
LHD 15	1513	6.1	341	29		1.8	388	<0.15	1.27	<0.1	50		<1	<0.1	60	<0.1	<0.1	303	242	<0.1	<0.1	1.62				1.02	2.01	40	19	1236	1555	11
LHD 17	402	5.3	330	57		1.0	178	<0.15	0.59	<0.1	29	<0.1	4.1	2.8	12	0.56	<0.1	83	157	<0.1	1.2	0.14	9.8	0.00049	2.92	0.04	3.57	76	22	1150	1416	−13
LHD 18	831	4.7	387	19		0.8	61	<0.15	0.29	0.22	39	1.6	4.1	1.0	29	0.58	<0.1	136	101	001	2.2	0.72	1.2	0.00036	1.65	0.99	0.60	135	18	1424	1510	47
LHD 23	9700	2.7	274	0		1.9	1559		<0.1	<0.1	1609	<0.1	3.2	9.4	173	5.00	6.4	1637	461	004	0.8	2.20	13.1	0.00702	1.22			355	24	1481	1693	12
LHD 28	4620	3.2	200	0		1.9	991	<0.15	2.57	<0.1	523		5.8	9.1	124	0.76	1.1	853	364	<0.1	<0.1	2.25				1.36	2.29			1750	1918	10

Concentrations are given in mg/l, electrical conductivity (EC) in µS/cm. Temperature (T) in °C is reservoir temperature obtained from borehole-measurements, gas phases in mmol/kg steam, Si as H_4SiO_4. "–" no measurement; green letters: acidic water, blue letters: neutral water.

Table 2 Hydrochemical composition of hot spring water

Sample name	EC (µS/cm)	pH	T (°C)	HCO_3^-	F^-	Cl^-	NO_2^-	Br^-	NO_3^-	SO_4^{2-}	PO_4^{3-}	Ca^{2+}	$Fe^{2+/3+}$	K^+	Mg^{2+}	Mn^{2+}	Na^+	H_4SiO_4	Sr^{2+}	Zn^{2+}	Li^{1+}	B^{3+}	Ba^{2+}	Al	Cs^{1+}	As	Ion balance (%)
M1	3865	2.1	82	0	0.93	27	<0.15	0.12	0.28	3047	4	123	236	23	40	2.03	40	155	0.18	0.84	0.03	0.449	0.001	57.5	0.004	0.044	−51
M2	2480	2.4	53	0	0.26	116	<0.1	0.37	0.12	653	2	14	14	17	5	0.58	110	55	0.05	<0.1	0.41	1.96	0.005	6.32	0.052	0.184	−24
M4	6880	1.8	66	0	1.22	2	<0.1	<0.1	<0.1	1936	<0.5	7	20	<10	5	0.40	<10	67	<0.1	<0.1	0.002				0.000	0.004	−93
M9	7835	2.0	57	0	0.45	2	<0.1	<0.1	<0.1	2985	<0.5	28	61	13	17	1.19	15	123	0.26	0.16							−80
M10	1291	2.7	80	0	0.62	20	<0.1	<0.1	<0.1	1517	<0.5	62	199	23	34	3.85	46	133	0.24	0.34							−28
M13	4640	2.4	61		0.36	1	<0.1	<0.1	<0.1	3236		149	251	<10	81	7.00	22	124	0.46	0.41					0.001	0.002	−45
M3	385	6.1	58	135	0.03	1	<0.1	<0.1	<0.1	104	<0.5	72	0.26	12	9	1.10	20	83	0.33	<0.1	0.01				0.002	0.017	5
M5	1156	6.6	47	186	0.29	122	<0.15	0.26	<0.1	102		77	0.75	20	39	0.55	98	67	0.19	<0.1	0.11				0.001	0.002	23
M6	452	7.0	41	104	1.19	21	<0.1	<0.1	<0.1	7		11	0.29	<10	5	0.39	78	58	<0.1	<0.1	0.11						30
M11	460	5.8	45		<0.1	4	<0.1	<0.1	1.17	151	<0.5	47	4.10	11	8	0.87	29	56	0.29	<0.1							35
M14	1228	6.7	45		0.24	121	<0.1	0.27	<0.1	80		77	<0.1	23	41	0.76	106	73	0.18	<0.1							

Concentrations are given in mg/l, electrical conductivity (EC) in µS/cm. Temperature (T) in °C is reservoir temperature obtained from borehole-measurements, gas phases in mmol/kg steam, Si as H_4SiO_4, "–" no measurement; green letters: acidic water, blue letters: neutral water.

Major ions in the acidic reservoir water are Cl, SO_4, Na, Si and K, with highest concentrations of Cl (991 to 1559 mg/l) and SO_4 (523 to 1609 mg/l; Table 1, 2). Neutral reservoir water mainly consists of Cl, SO_4, HCO_3, Na, Si and K (Table 1, 2). Cl ranges between 12 and 452 mg/l, SO_4 between 17 and 114 mg/l, and HCO_3 between 6 and 68 mg/l. Main gas phases are CO_2 and H_2S with up to 355 mmol/kg (Table 1, 2).

Major ions in acidic springs are SO_4 (653 to 3236 mg/l), Fe (14 to 251 mg/l), Ca and Si. Neutral spring water mainly consists of HCO_3 (104 to 186 mg/l), SO_4 (7 to 151 mg/l), Cl, Na, Si and Ca (Table 1,2).

Ternary *Giggenbach-diagrams* displays the relation between Cl, SO_4 and HCO_3 concentrations in geothermal waters (Giggenbach 1988). Plotting the samples from the Lahendong geothermal field reveals two types of reservoir- and hot spring waters (Fig. 2). There are neutral reservoir samples showing mostly high Cl concentrations, while the acidic reservoir waters are predominantly volcanic waters with high SO_4 concentrations. Neutral springs with high Cl and HCO_3 concentrations host peripheral water, while acidic springs host volcanic water (Fig. 2).

The correlations of pH with SO_4 and of Cl with boron (B) reveal a clear separation of acidic and neutral waters (Fig. 3). In the Cl/B-plot three water types can be differentiated. The most neutral waters show a linear trend with low B concentrations (1–4 mg/l). Wells LHD 8 and LHD 17 are marked by higher B concentration, LHD 23 showing the highest Cl and B concentration as well as the highest Cl/B ratio. The lowest concentrations were measured in well LHD 5 (Fig. 3).

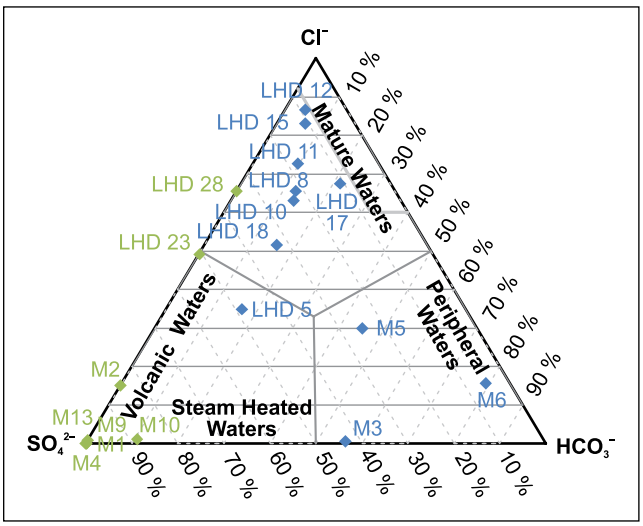

Fig. 2 Giggenbach-diagram correlating relative Cl, SO_4, and HCO_3 concentrations for well and spring water. *Green labels*: acidic water, *blue labels*: neutral water. Concentrations are given in Table 1, 2

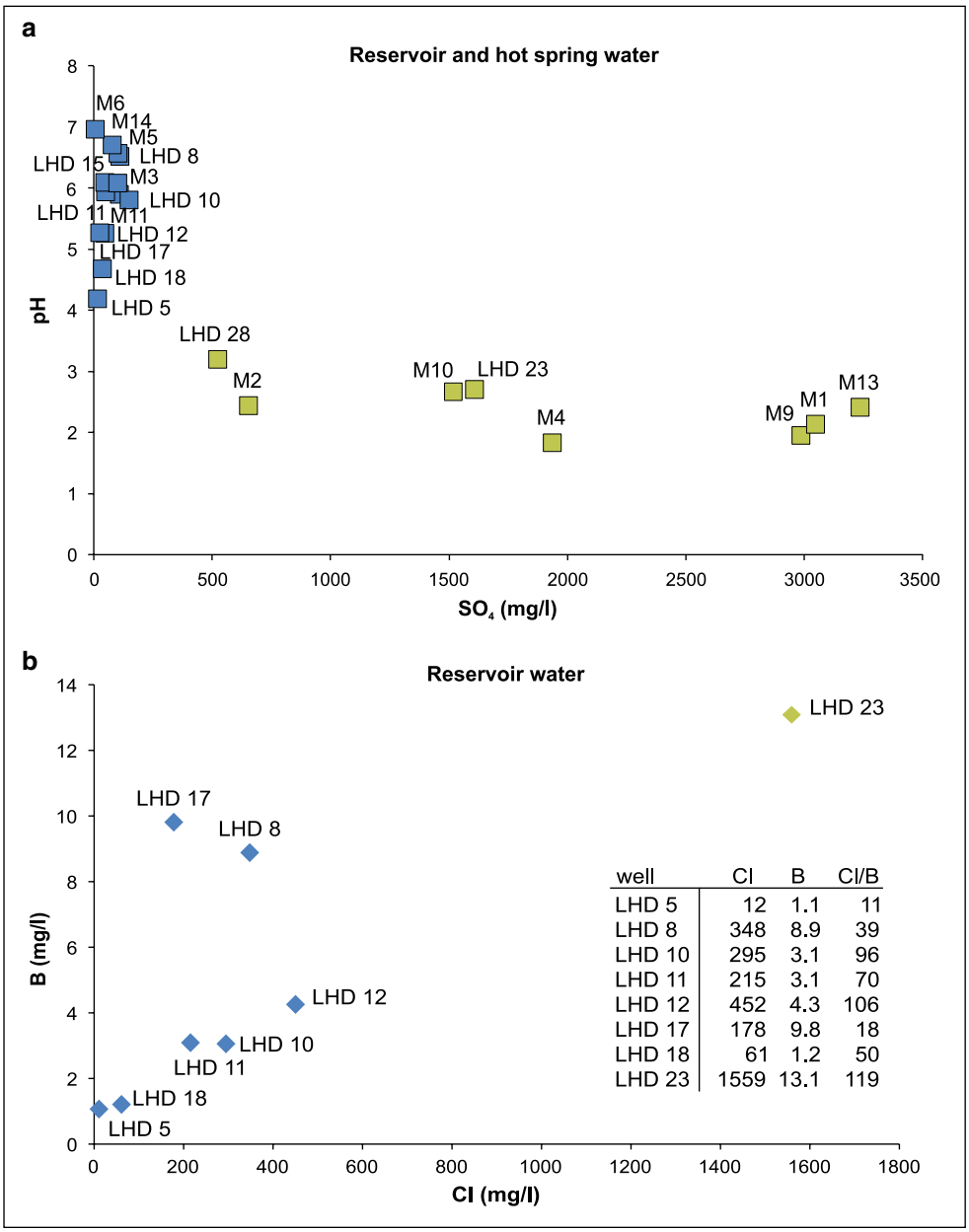

Fig. 3 **a** Plot of pH against SO_4 for reservoir and hot spring water samples; **b** Correlation of B with Cl of reservoir water with respective concentrations and ratios. *Green labels*: acidic water, *blue labels*: neutral water, concentrations in mg/l

Rocks

Rock specimen, collected from reservoir well-cores and from surface outcrop, were analyzed for their chemical and mineral composition. Special attention was also paid to occurrence of fluid flow pathways in the form of fractures.

The Lahendong reservoir is predominantly composed of andesite and volcanic breccia. Results from XRD and visual analysis indicate predominantly altered and unaltered plagioclase, quartz, epidote, pyroxene and olivine in the andesites (Fig. 4 a-2). The volcanic breccia consists of various rock fragments and minerals (e.g. plagioclase, quartz), hosted in a microcrystalline matrix (Fig. 4 a-2). Hydrothermally altered minerals appear colorful in thin sections under crossed nicols light, altered quartz and feldspars in bright tints, pyroxenes in greens and pink (Fig. 4 b-2, b-4).

Pores and veins within the reservoir rocks can act as fluid pathways (e.g. Figure 4 a-1, b-3). These veins are often filled by secondary minerals, obvious in visual (Fig. 4 a-4) and microscopic analysis of thin sections (Fig. 4 b-4). The minerals filling the veins were characterized by XRD and rock cuttings as phyllosilicates (e.g. chlorite and clay minerals). They are more abundant in rocks hosting acidic water (Table 3, 4, 5, 6, 7).

The surface sample GS9 is an unaltered andesite consisting predominantly of plagioclase, diopside, and forsterite (Fig. 4c). Other rocks collected at other hot springs mainly contain quartz and albite (samples M3 and M4; Hernan-

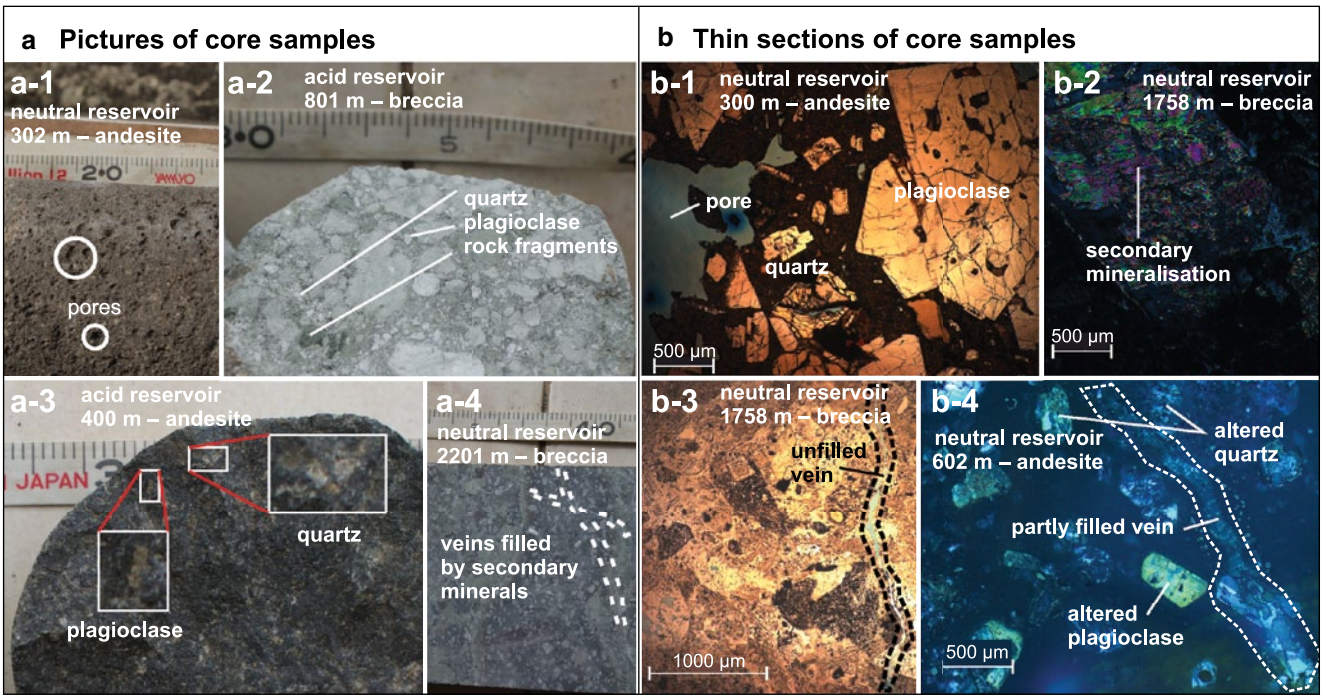

Fig. 4 **a** Photographs of core samples from geothermal wells representing different rock types (breccia and andesite) with their main components (a-2 and a-3) and examples for porosity (a-1 and a-4), and **b** Thin sections of core samples showing unaltered (b-1 and b-3) to highly altered minerals (b-2 and b-4) as well as types of fluid pathways (pores and veins); **c** XRD patterns from surface rock samples. GS9 as example for unaltered andesite, GS5-1, 5-3, GS15-A, M3 and M4 are highly altered samples with main phases as indicated

dez Castaneda; 2014). Samples GS5-1, GS5-3, GS5-5, and GS15-A represent altered rock material from manifestations hosting acidic hot springs and fumaroles. These latter samples often show elemental sulphur (GS5-1) and clay mineral such as kaolinite (GS15-A) as alteration products (Fig. 4c). Further alteration minerals detected are goethite, antigorite and alunite (observed in GS5-3 and GS5-5). Traces of rutile are seen in XRF data, where the chemical content of whole rocks shows 1.45 % of TiO_2 (Table 5). It appears most likely as a relict from pre-altered rock (Fig. 4c).

Permeability

Permeability has been separately averaged for each of the three rock types—andesite, volcanic breccia, and tuff. Andesite samples have a permeability of ~ 2.08E-15 m^2, lying between tuff with the lowest permeability (~ 1.97E-15 m^2) and volcanic breccia as the highest (2.32E-14 m^2). These reflect values typical for low permeable fractured igneous rocks (Schön 2004).

Core samples from the geothermal wells of course represent more intact, less altered reservoir rocks as compared to outcrops. Nevertheless, some cores were crumbly or showed fracture filling and secondary mineralization (Table 8).

Geochemical model

Modeling with PHREEQC predicted potential mineral precipitation depending on pressure and temperature conditions. After the first modeling step—which equilibrated the reservoir water with the main gas phases at the physical reservoir conditions—muscovite, kaolinite, pyrite, sulphur, chalcedony/quartz, alunite, and gibbsite were found to be supersaturated (Table 6). After the second step when reservoir water was equilibrated with these minerals, only the acidic reservoir water (LHD23) still remained supersaturated with respect to phyllosilicates such as chlorite, chrysotile or talc.

The hydrochemical simulation of hot spring water was performed by cooling and degassing of reservoir water and mixing with cold diluted water. Then the water was equilibrated with previously supersaturated SiO_2 minerals. The resulting water was still supersaturated with a variety of mineral phases, dominated by chlorite, muscovite, silica-minerals (chrysotile, talc) and pyrite (Table 7). The modeling suggests that spring water forms by mixing of high T and salinity reservoir waters with near-surface low T and salinity waters. The neutral springs M3 and M11, which show lower salinities and higher SO_4 concentrations than the reservoir water, derive directly from the surface. The springs M5, M6, and M14 discharge in the geothermal outflow zone and show higher salinities, due to high Cl concentrations.

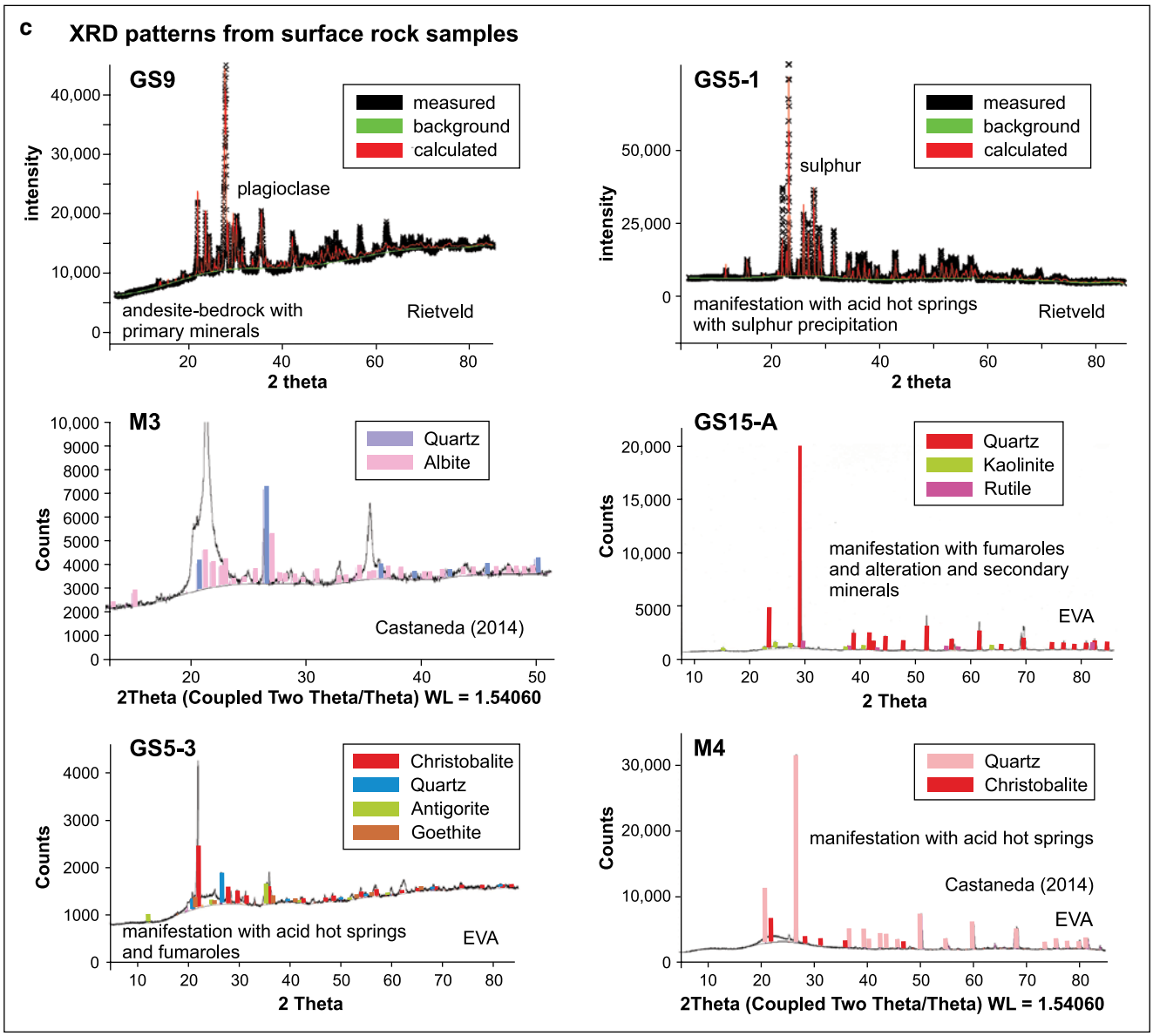

Fig. 4 continued

Discussion

Characterizing fault zones in geothermal systems plays a key role in improving reservoir performance. As faults might behave as both barriers and conductors of fluids, they basically dominate subsurface fluid flow processes (Moeck and Dussel 2007). The mechanical interaction between faults and fluids has been shown also by high-resolution seismological experiments (Kwiatek et al., 2014). Flow rates determine the retention period of fluids in the reservoir rock, which significantly affects the water-rock interaction. Water-rock interaction, in turn, is one of the main processes responsible for the geochemical and mineralogical properties of the reservoir (Arnorsson 2000). In areas of extensive fluid flow, such as along permeable fault zones, a distinct change of geochemistry can be observed. Turning this association around, geochemical properties can then be used to locate and characterize fault zones. Here we discuss several examples that exemplify the ability to trace fault zone permeability using geochemical "tracers".

In the Lahendong reservoir, vertical faults appear to act as barriers for flow in the horizontal direction, preventing fluids on either side from mixing with each other. These faults represent the boundary between the acidic and neutral water reservoir compartments (Fig. 1, 5). On the other hand, faults also open pathways for fluids rising towards the surface. On the surface, hot springs are located at fault exposures, especially at fault intersections. This is the case

Table 3 Reservoir rock composition from core samples

Core samples	Analysis method	Major mineral phases
Neutral reservoir (LHD2,4,5,7)	Cores, thin sections	Quartz, plagioclase, olivine, biotite, pyroxene, epidote, pyrite, muscovite
Acid reservoir (LHD1)	Cores, thin sections	Quartz, plagioclase, pyroxene, biotite, epidote, muscovite
Acid reservoir (LHD23,24,28)	XRD, Pertamina Geothermal Energy (2009), Cutting-Report	Quartz, plagioclase, chlorite, pyrite, clay (smectite, illite), epidote, muscovite

Table 4 Surface rock composition from XRD analysis

Surface rock samples	Rock type	XRD Refinement method	Major mineral phases
GS 5-1 (manifestation with acid springs)	Altered material	Rietveld	Sulphur
GS 5-3 (manifestation with acid springs)	Red alteration on andesite	EVA	Christobalite, quartz, antigorite, goethite
GS 5-5 (manifestation with acid springs)	Green alteration on andesite	EVA	Christobalite, alunite
GS 9 (unaltered andesite)	Unaltered andesite	Rietveld	Plagioclase
GS 15-A (manifestation with fumaroles)	Highly altered material	EVA	Quartz, kaolinite, rutile
M3 (manifestation with neutral springs)	Highly altered material	Hernandez Castaneda (2014)	Quartz, albite
M4 (manifestation with acid springs)	Highly altered material	Hernandez Castaneda (2014)	Christobalite, quartz

for the acidic springs that appear on top of the acidic section of the reservoir (Fig. 1).

Deep acidic water typically forms as a consequence of H_2S degassing from a magma chamber. This takes place after the sulfide oxidizes to sulfate by O_2 dissolved in the surface meteoric waters (Nicholson 1993). In the study area, the magma chamber is assumed to be located beneath Lake Linau (Brehme et al. 2014). Here, meteoric water infiltrates through faults and oxidizes the magmatic H_2S. This lowers the pH-value and increases the SO_4 content, as has been described for the Alto Peak geothermal system in the Philippines (Reyes et al. 1993). There, where the vertical permeability is also controlled by faults/fractures, faults allow the infiltration of cooler groundwater and the consequent reaction with H_2S.

Some acidic springs, such as M9 and M13, are located at off-fault spots (Fig. 1). Their occurrence is not likely related to permeable fault zones, but to steam-heated zones, where the shallow groundwater is heated and acidified by rising gases. In steam-heated springs, pH and Cl-concentrations are typically significantly lower. The acidic water dissolves minerals, especially metals, from the volcanic host rocks leading to increased Fe-, Mn- and Al-concentrations (Arnorsson et al. 2007). Similarly to the Lahendong geothermal field, steam-heated springs in the Patuha geothermal field in Java, Indonesia, that are also located off the center of the field, also have increased Mn, Al and Cr concentrations (Sriwana et al. 2000).

Other indications of the water origins are the Cl and B concentrations. In thermally heated water, these concentrations are much higher compared to fresh cold water. This due to increased water-rock interactions of thermally heated water in the reservoir (Arnorsson 1985). In the Lahendong reservoir, well LHD 23 produces water with a Cl concentration of 1559 mg/l and a B concentration of 13.1 mg/l. All other neutral water wells show lower concentrations of Cl and B. The lowest Cl and B concentrations were measured at well "LHD 5" (Fig. 3b). The water produced at this well is diluted with cold surface-near groundwater infiltrating through a nearby fault connected to the reservoir (Fig. 5; Brehme et al. 2014). A similar trend can be observed for correlation of the electrical conductivity with Cl and B concentrations, which is because Cl is the dominating conducting anion in water composition. These observations indicate that the compositions and the locations of Lahendong reservoir waters are controlled by fluid flow along the vertically permeable fault zones.

Faults and fractures in reservoir also affect its temperature and productivity. In Lahendong, the northern section of the reservoir is about 60 °C cooler than the southern section—264 versus 319 °C—while its productivity is five times higher. Some individual northern wells produce 20

Table 5 XRF analysis from selected surface samples

Sample	SiO_2	TiO_2	Al_2O_3	Fe_2O_3	MnO	MgO	CaO	Na_2O	K_2O	P_2O_5	Total
GS 5-3	65.4	1.222	11.0	7.62	0.07	1.83	0.93	0.18	0.18	0.120	99.2
GS 5-5	81.8	1.095	6.9	0.27	<0.01	0.01	0.10	0.09	1.17	0.161	99.1
GS15-A	79.8	1.448	7.4	1.95	0.02	0.14	0.15	<0.01	0.22	0.076	99.2

Table 6 PHREEQC calculations of equilibrated and supersaturated minerals in reservoir water

Sample	In first step supersaturated mineral phases (SI)	Reservoir T (°C)	Reservoir p (bar)	Gas Phases (mmol/kg steam)	In final step supersaturated mineral phases (SI)
Neutral reservoir	Muscovite (3), pyrite (3), kaolinite (1), sulphur (0.9), gibbsite (0.4), quartz (0.3), chalcedony (0.14)	232–387	89–159	40–135 CO_2 9–30 H_2S	–
Acid reservoir	Muscovite (5), pyrite (4), kaolinite (1), alunite (0.9), sulphur (0.8), gibbsite (0.7)	200–274	121–139	356 CO_2 24 H_2S	chlorite (5.53), chrysotile (0.16), talc (5.04)

SI Saturation Index, locations see Fig. 1

Table 7 PHREEQC calculations of equilibrated and supersaturated minerals in hot spring water

Sample	In first step equilibrated mineral phases (SI)	In final step supersaturated mineral phases (SI)
Neutral springs	Quartz (1.4), chalcedony (1), amorphous silica (0.16)	Albite, anorthite, aragonite, calcite, chlorite (11), chrysotile, dolomite, fluorite, goethite, hematite (8), illite, k-feldspar, muscovite (11), mackinawite, pyrite, quartz, rhodochrosite, talc (7)
Acid springs	Quartz (1.8), chalcedony (1.3), amorphous silica (0.5)	Albite, anorthite, aragonite, ca- montmorillonite, calcite, chlorite (22), chrysotile (11), dolomite, fluorite, gibbsite, goethite, hematite, illite, k-feldspar, muscovite (7), kaolinite, mackinawite, pyrite (7), quartz, siderite, talc (15)

SI Saturation Index, locations see Fig. 1

Table 8 Permeability values of selected wellbore-core samples, locations see Fig. 1

Sample	Rock type	Observed alteration pattern	Matrix–Permeability (m^2)
LHD1 801–802	B		1.53E–14
LHD1 1000–1001	T	X	8.90E–16
LHD1 2100–2101	T		3.31E–15
LHD2 300–302	A	X	6.11E–14
LHD3 2201–2203	B		1.49E–14
LHD4 652–653	B		1.26E–14
LHD4 850–852	A		2.25E–14
LHD4 1001–1002	B	X	6.82E–14
LHD4 2304–2305	A		3.38E–16
LHD5 602–603	B		1.12E–14
LHD5 752–753	A		1.08E–16
LHD5 1102–1103	A		7.88E–14
LHD5 1404–1406	A		2.95E–15
LHD5 1575–1576	A	X	7.92E–18
LHD7 901–902,3	A	X	7.15E–16
LHD7 1567.8–1568	T		1.70E–15
LHD7 1756–1758	B		1.68E–14
Average values	**Andesite (A)**		**2.08E–15**
	Breccia (B)		**2.32E–14**
	Tuff (T)		**1.97E–15**

MW_e, compared to five wells needed to produce a net of 20 MW_e in the south. Despite the lower temperature, the substantially higher productivity is probably due to the presence of vertically permeable fractures that increase fluid flow. These fractures allow infiltration of cold surface water into the reservoir, which leads to lower reservoir temperatures in this particular area (Fig. 5).

Another important process controlling the properties in a geothermal reservoir is the interaction between water and rocks (Browne 1970). The main requirements for vigorous reactions are fluid types and enhanced fluid flow, specific rock types, and physico-chemical conditions. Rock hosting the acidic water in Lahendong contain more sulphur and clay minerals. Numerical modeling results confirmed that the pH value of the reservoir water plays the dominant role with respect to chemical reactions since the acidic water alters the host rock more effectively (Fig. 5).

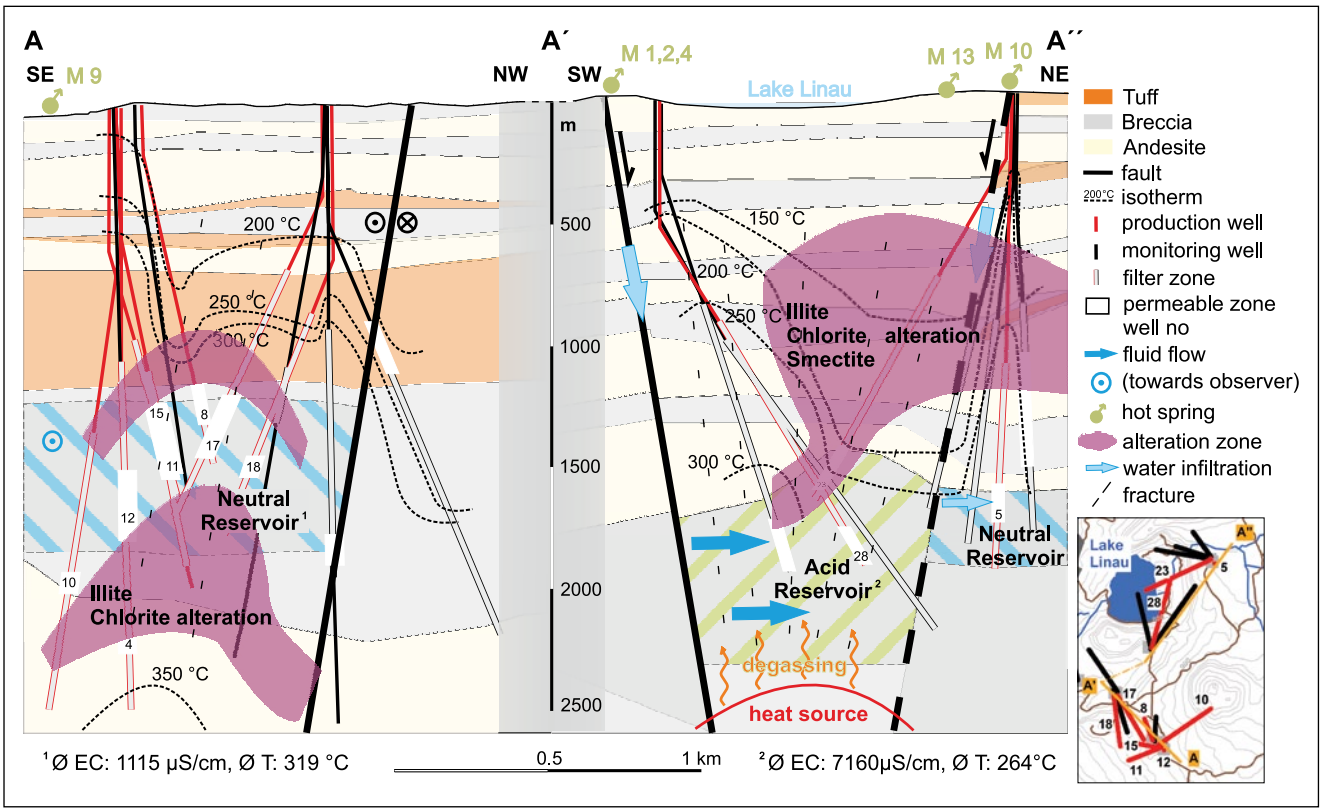

Fig. 5 Conceptual geochemical model of the study area, described by cross-sections with geological layering, fault location, temperature distribution, sample points and alteration patterns. For cross section line see Fig. 1 (modified after Brehme et al. 2014 and Utami 2011)

Phyllosilicates, such as chlorite, mica, kaolinite, smectite and illite, formed as products of hydrothermal alteration of primarily abundant feldspar by acidic waters (Table 3, 4, 5, 6, 7). These secondary minerals are apparently more stable at the given conditions (John 2007; Utami 2011). Mineral modifications have been intensively studied in the Lahendong geothermal field by Utami (2011) and Utami et al. (2004). Two alteration types were observed: replacement and direct deposition. While chlorite appears as replacement of plagioclase, illite precipitated from circulating fluids. Generally, alteration patterns are widespread in the acidic and highly fractured northern section of the reservoir (Utami 2011; Fig. 5).

In summary, rock alteration is mainly controlled by water-rock-interaction in highly fractured and permeable areas accommodating increased fluid flow. However, at a later stage, the alteration process of the host rock decreases permeability again by filling of fractures with secondary minerals. This effect has been indirectly observed in wellbore-core samples of the study area. In faulted areas with high fracture density, fewer cores were available because the reservoir rocks were highly damaged thus limiting core extraction. The few available cores showing alteration were of very low permeability. Secondary mineralization, which fills the fluid pathways in fractured areas, can also clog perforated casings. This may lead to a decrease of well productivity as observed in the Patuha geothermal field (Layman and Soemarinda 2003)—a major risk for geothermal plant operation.

Further processes controlling the fluid flow and phase change in the Lahendong system are degassing and boiling due to pressure release. Degassing was mainly observed in the northern section of the acidic reservoir. This area hosts the highest CO_2 and H_2S concentrations, as measured in discharge at well LHD 23. Gas discharge was observed at the surface at several fumaroles around Lake Linau. Furthermore, increased electrical conductivities have been measured in fluids of the northern section of the reservoir (Table 8). This can be explained by subsurface boiling, a process that evaporates water and transports the heat of the geothermal fluid upward and out of the reservoir (Arnorsson 2000). The increased electrical conductivity could therefore indicate the location of low temperature regions in the area.

In the Lahendong hydraulic conductivities of fault zones strongly influence geochemical reservoir characteristics. The observations described here show that the permeability controls fluid flow and the distribution of water types. The fluid flow in fractures influences the reservoir-temperature, the alteration degree of host rocks, and the productivity of the geothermal field. Degassing and water-rock-interaction were identified as the main processes controlling the fluid flow and phase change in this environment.

Conclusion

In this study, geochemical data from the Lahendong geothermal site were collected and interpreted in the context with the hydraulic conductivity of fault zones. The geochemical properties investigated were fluid-and-rock compositions and their interactions. These properties depend strongly on fluid flow rates, which is increased in high permeable areas.

In the study area, two reservoir sections reflecting different geochemical properties suggest the presence of an impermeable fault zone. This zone appears to be a vertical boundary separating a northern area with acidic brine, considerable gas discharge, high productivity, and strongly altered rocks from a southern section hosting neutral water, higher temperatures, and less altered rocks. The fluid flow and geochemical reactions were found to be mainly controlled by the permeability in fault-related fractures. In these permeable areas fluid flow increases and causes rise of fluids at such vertically permeable spots. Eventually the increased chemical activity results in limited-permeability rocks. Thus investigating alteration-related permeability distributions along a geothermal reservoir is crucial for site selection and smart drilling strategies. These types of studies help support a sustainable geothermal exploitation program, avoiding risks such as low-productive wells or the production of highly corrosive waters.

Acknowledgments The authors acknowledge the continuous support within the team of the International Centre for Geothermal Research. We thank S. Tonn and K. Günther for fluid-analyses, R. Naumann, A. Gottsche, H. Liep and M. Ospald for geochemical analyses and Dr. F. Bulut for remarks on the manuscript. We would like to thank Dr. H. Milsch, B. Peters and D. Otten for helping at the Gas-Permeameter. Prof. M. Hochstein is greatly acknowledged for continuous fruitful discussions, which made this study possible. M. Andhika supported this work with assisting in communication in Indonesia and continuos discussion on the topic. I am deeply grateful to Prof. P. Malin, who reviewed the manuscript and took care of linguistic issues. Giggenbach-diagrams have been done with the help of an excel-sheet provided by Powell and Cumming (2010).

References

Appelo, C.A.J.: Principles , caveats and improvements in databases for calculating hydrogeochemical reactions in saline waters from 0 to 200 ° C and 1 to 1000 atm. Appl. Geochemistry 55, 62–71 (2015)

Arnorsson, S.: The use of mixing models and chemical geothermometers for estimating underground temperatures in geothermal systems. J. Volcanol. Geotherm. Res. **23**, 299–335 (1985)

Arnorsson, S.: Arnorsson-Isotopic and chemical techniques in geothermal exploration, development and use. Report, International Atomic Energy Agency, Vienna (2000)

Arnorsson, S., Stefansson, A., Bjarnason, J.O.: Fluid-Fluid Interactions in Geothermal Systems. Rev. Mineral. Geochem. **65**, 259–312 (2007). doi:10.2138/rmg.2007.65.9

Belsky, A., Hellenbrandt, M., Karen, V.L., Luksch, P.: New developments in the Inorganic Crystal Structure Database (ICSD): accessibility in support of materials research and design. Acta Crystallogr. B. **58**, 364–369 (2002) doi:10.1107/S0108768102006948

Bergerhof, G., Brown, I.D.: Inorganic crystal structure database. Chrystallographic Database, International Union of Chrystallography (1987)

Brehme, M., Scheytt, T., Çelik, M., Dokuz, U.E.: Hydrochemical characterisation of ground and surface water at Dörtyol/Hatay/Turkey. Environ. Earth Sci. **63**, 1395–1408 (2010). doi:10.1007/s12665-010-0810-1

Brehme, M., Haase, C., Regenspurg, S., Moeck, I., Deon, F., Wiegand, B.A., Kamah, Y., Zimmermann, G., Sauter, M.: Hydrochemical patterns in a structurally controlled geothermal system. Mineral. Mag. **77**, 767 (2013) doi:10.1180/minmag.2013.077.5.2

Brehme, M., Moeck, I., Kamah, Y., Zimmermann, G., Sauter, M.: A hydrotectonic model of a geothermal reservoir—A study in Lahendong, Indonesia. Geothermics **51**, 228–239 (2014). doi:10.1016/j.geothermics.2014.01.010

Browne, P.R.L.: Hydrothermal alteration as an aid in investigating geothermal fields. Geothermics. **2**, 564–570 (1970) doi:10.1016/0375â6505(70)90057-X

Corsi, R.: Scaling and corrosion in geothermal equipment: problems and preventive measures. Geothermics. **15**, 839–856 (1986)

Deon, F., Regenspurg, S., Zimmermann, G.: Geothermics Geochemical interactions of Al2O3 -based proppants with highly saline geothermal brines at simulated in situ temperature conditions. Geothermics. **47**, 53–60 (2013)

Deon, F., Förster, H.-J., Brehme, M., Wiegand, B., Scheytt, T., Moeck, I., Jaya, M.S., Putriatni, D.J.: Geochemical/hydrochemical evaluation of the geothermal potential of the Lamongan volcanic field (Eastern Java, Indonesia). Geotherm. Energy. **3**, 20 (2015)

Ellis, A.J., Mahon, W.A.J.: Chemistry and geothermal systems. Academic Press Inc, New York (1977)

Giencke, J.: Introduction to EVA. Bruker Cooperation, Billerica (2007)

Giggenbach, W.F.: Geothermal solute equilibria. Derivation of Na-K-Mg-Ca geoindicators. Geochim. Cosmochim. Acta. **52**, 2749–2765 (1988). doi:10.1016/0016-7037(88)90143-3

Hernandez Castaneda, M.C.: Characterization of silica precipitates formed at geothermal conditions. Universität Freiburg, Freiburg im Breisgau (2014)

John, L.: Hydrothermal alteration mineralogy in geothermal fields with case examples from Olkaria Domes geothermal field, Kenya. Report, UNU-GTP (2007)

Koestono, H.: Lahendong Geothermal Field, Indonesia: Geothermal model based on wells LHD-23 and LHD-28. Master-Thesis at University of Iceland (2010)

Kwiatek, G., Bulut, F., Bohnhoff, M., Dresen, G., Oates, S., Santos, P. A.: High-resolution analysis of seismicity induced at Berlín geothermal field, El Salvador, (2013). Geothermics, doi: 10.1016/j.geothermics.2013.09.008

Larson, A.C., Von Dreele, R.B.: GSAS—General Structure Analysis System. Los Alamos National Laboratory Report LAUR 86–748, University of California (2004)

Layman, E., Soemarinda, S.: The Patuha Vapor-Dominated Resource West Java, Indonesia. Proceedings of the 28th Workshop on Geothermal Reservoir Engineering, pp. 56–65. Stanford University, Stanford (2003)

Milsch, H., Priegnitz, M., Blöcher, G.: Permeability of gypsum samples dehydrated in air. Geophys. Res. Lett. 38, 6 (2011). doi:10.1029/2011GL048797

Moeck, I., Dussel, M.: Fracture networks in Jurassic carbonate rock of the Algarve Basin (South Portugal): Implications for aquifer behaviour related to the recent stress field. IHA Sel. Pap. Ser. 9, 479–488 (2007)

Nicholson, K.: Geothermal fluids—chemistry and exploration techniques. Springer, Berlin (1993)

Powell, T., Cumming, W.: Spreadsheets for geothermal water and gas geochemistry. Proceedings of the 35th Workshop on Geothermal Reservoir Engineering. Stanford University, Stanford (2010)

Parkurst, D., Thorstenson, D., Plummer, L.: PHREEQE, a computer program for geochemical calculations, US Geological Survey Water. Report, USGS (1980)

Parkhurst, D., Appelo, C.A.J.: Description of Input and Examples for PHREEQC Version 3a Computer Program for Speciation, Batch-reaction, One-dimensional Transport, and Inverse Geochemical Calculations. Model. Tech. B. 6 497 (2013)

Robinson, D., Peng, D., Chung, S.: The development of the Peng-Robinson equation and its application to phase equilibrium in a system containing methanol. Fluid Phase Equilib. **24**, 25–41 (1985). doi:10.1016/0378-3812(85)87035-7

Reyes, A., Giggenbach, W., Saleras, J.: Petrology and Geochemistry of Alto Peak, a Vapor-cored Hydrothermal System, Leyte Province, Philippines. Geothermics **22**, 479–519 (1993)

Schön, J.H.: Physical properties of rocks. Elsevier Ltd., Amsterdam (2004)

Siahaan, E.E., Soemarinda, S., Fauzi, A., Silitonga, T., Azimudin, T., Raharjo, I.B.: Tectonism and Volcanism Study in the Minahasa Compartment of the North Arm of Sulawesi Related to Lahendong Geothermal Field, Indonesia, in: Proceedings World Geothermal Congress 2005, Antalya, Turkey, 24–29 April 2005 (2005)

Sriwana, T., van Bergen, M.J., Varekamp, J.C., Sumarti, S., Takano, B., van Os, B.J.H., Leng, M.J.: Geochemistry of the acid Kawah Putih lake, Patuha Volcano, West Java, Indonesia. J. Volcanol. Geotherm. Res. **97**, 77–104 (2000). doi:10.1016/S0377-0273(99)00178-X

Surachman, S., Tandirerung, S.A., Buntaran, T., Robert, D.: Assessment of the Lahendong geothermal field, North Sulawesi, Indonesia, in: Proceeding Indonesian Petroleum Association, Sixteenth Annual Convention, October 1987. pp. 385–398 (1987)

Tanikawa, W., Shimamoto, T.: Comparison of Klinkenberg-corrected gas permeability and water permeability in sedimentary rocks. Int. J. Rock Mech. Min. Sci. **46**, 229–238 (2009). doi:10.1016/j.ijrmms.2008.03.004

Toby, B.: EXPGUI, a graphical user interface for GSAS. J. Appl. Crystallogr. **34**, 210–213 (2001)

Truesdell, A.H., Stallard, M.L., Trujillo, P.E., Counce, D., Janik, C.J., Winnett, T.L., Goff, F., Shevenell, L.: Interpretation of fluid chemistry from the PLTG-1 exploratory drill hole, Platanares. Honduras. Geotherm. Resour. Counc. Transactions. **11**, 217–222 (1987)

Utami, P.: Hydrothermal alteration and the evolution of the Lahendong geothermal system, North Sulawesi, Indonesia. Dissertation, University of Auckland, Auckland (2011)

Utami, P., Siahaan, E.E., Azimudin, T., Browne, P.R.L., Simmons, S.F.: Overview of the Lahendong geothermal field, North Sulawesi, Indonesia: A progress report, in: Proceedings of the 26th NZ Geothermal Workshop 2004. pp. 1–6 (2004)

White, D.E.: Thermal Water of Volcanic origin. Bull. Geol. Soc. Am. **68**, 1637–1658 (1957)

Wiegand, B.A., Brehme, M., Teuku, F., Amran, I.A., Prasetio, R., Kamah, Y., Sauter, M.: Geochemical and isotopic investigation of fluids from Lahendong geothermal field. Mineral. Mag. **77**, 2491 (2013). doi:10.1180/minmag.2013.077.5.23